

RESEARCH LETTER

10.1002/2015GL066882

Key Points:

- Fault mirrors in the studied fault zones are composed of silica gel and melt patches
- Melt patches were generated in small fast slip by flash heating
- Fault mirrors represent fossils of small earthquakes

Supporting Information:

- Supporting Information S1

Correspondence to:

L.-W. Kuo,
liweikuo@ncu.edu.tw;
liweikuo@gmail.com

Citation:

Kuo, L.-W., S.-R. Song, J. Suppe, and E.-C. Yeh (2016), Fault mirrors in seismically active fault zones: A fossil of small earthquakes at shallow depths, *Geophys. Res. Lett.*, 43, doi:10.1002/2015GL066882.

Received 4 NOV 2015

Accepted 4 JAN 2016

Accepted article online 7 JAN 2016

Fault mirrors in seismically active fault zones: A fossil of small earthquakes at shallow depths

Li-Wei Kuo¹, Sheng-Rong Song², John Suppe², and En-Chao Yeh³

¹Department of Earth Sciences, National Central University, Taoyuan, Taiwan, ²Department of Geosciences, National Taiwan University, Taipei, Taiwan, ³Department of Earth Sciences, National Taiwan Normal University, Taipei, Taiwan

Abstract Fault mirrors (FMs) are naturally polished and glossy fault slip surfaces that can record seismic deformation at shallow depths. They are important for investigating the processes controlling dynamic fault slip. We characterize FMs in borehole samples from the hanging wall damage zone of the active Hsiao-tung-shi reverse fault, Taiwan. Here we report the first documented occurrence of the combination of silica gel and melt patches coating FMs, with the silica gel resembling those observed on experimentally formed FMs that were cataclastically generated. In addition, the melt patches, which are unambiguous indicators of coseismic slip, suggest that the natural FMs were produced at seismic rates, presumably resulting from flash heating at asperities on the slip surfaces. Since flash heating is efficient at small slip, we propose that these natural FMs represent fossils of small earthquakes, formed in either coseismic faulting and folding or aftershock deformation in the active Taiwan fold-and-thrust belt.

1. Introduction

A number of physical and chemical mechanisms have been proposed to result in fault lubrication during earthquakes, based on both experimental data and theoretical considerations (e.g., flash heating of asperities, frictional melting, silica gel, nanopowder, and thermal decomposition) and are postulated to occur on natural faults (see *Di Toro et al.* [2011] and *Niemeijer et al.* [2012] for a summary). Solidified frictional melts, or pseudotachylytes, have been documented both in nature [e.g., *Sibson*, 1975; *Swanson*, 1992; *Camacho et al.*, 1995; *Di Toro and Pennacchioni*, 2005] and in experiments [*Spray*, 1987; *Tsutsumi and Shimamoto*, 1997] and are commonly recognized as fossil earthquakes [*Sibson*, 1975; *Di Toro et al.*, 2006]. Pseudotachylyte therefore has been used in many settings to infer the seismic nature of fault zones and allows the retrieval of key parameters related to the earthquake source [e.g., *Di Toro et al.*, 2009]. However, with the exception of frictional melting evidence [*Allen*, 2005; *Di Toro et al.*, 2006], only a few other potential indicators of seismic slip have been observed in nature [*Kirkpatrick et al.*, 2013; *Siman-Tov et al.*, 2013; *Smith et al.*, 2013], which is a severe limitation in our understanding of earthquake physics.

Other proposed geologic evidence for seismic slip includes the combination of carbonate dissociation and fluid-rock interaction [*Rowe et al.*, 2012a], thermally altered biomarkers [*Polissar et al.*, 2011; *Savage et al.*, 2014], thermally altered magnetic minerals [*Evans et al.*, 2014], peculiar crystal-plastic features [*Smith et al.*, 2013], injection of fluidized gouge [*Rowe et al.*, 2012b], and fault mirrors (FMs) [*Fondriest et al.*, 2013; *Siman-Tov et al.*, 2013]. Fault mirrors (FMs) have been shown experimentally to form at seismic rates accompanied with thermal decomposition, nanograin coating and sintering, or recrystallization reaction [*Han et al.*, 2007; *Fondriest et al.*, 2013; *Smith et al.*, 2013; *Siman-Tov et al.*, 2015] and also have been reported from exhumed fault zones both in carbonate and in silicate host rocks [*Power and Tullis*, 1989; *Collettini et al.*, 2013; *Siman-Tov et al.*, 2013; *Fondriest et al.*, 2015]. The FMs with truncated and exploded grains in carbonate host rock provide criteria for seismic slip [*Fondriest et al.*, 2015], but these in silicate-hosted faults remain largely unknown, and so other evidence and the associated mechanism for seismic slip must be identified.

Here we report about the first documented observations of FMs associated to silica gel and pseudotachylytes in silicate-hosted rocks. The FMs were found in borehole cores retrieved from the hanging wall damage zone of the Hsiao-tung-shi active reverse fault, Taiwan [*Shyu et al.*, 2005]. In an effort to understand FMs in silicate-hosted faults and the associated process, we examine the mineralogy and the macrostructure and microstructure of the FMs, discuss possible mechanism for the FMs formation, address the geological record of the seismically active fault and fold, and, by extension, other tectonically active regions with incomplete earthquake catalogues.

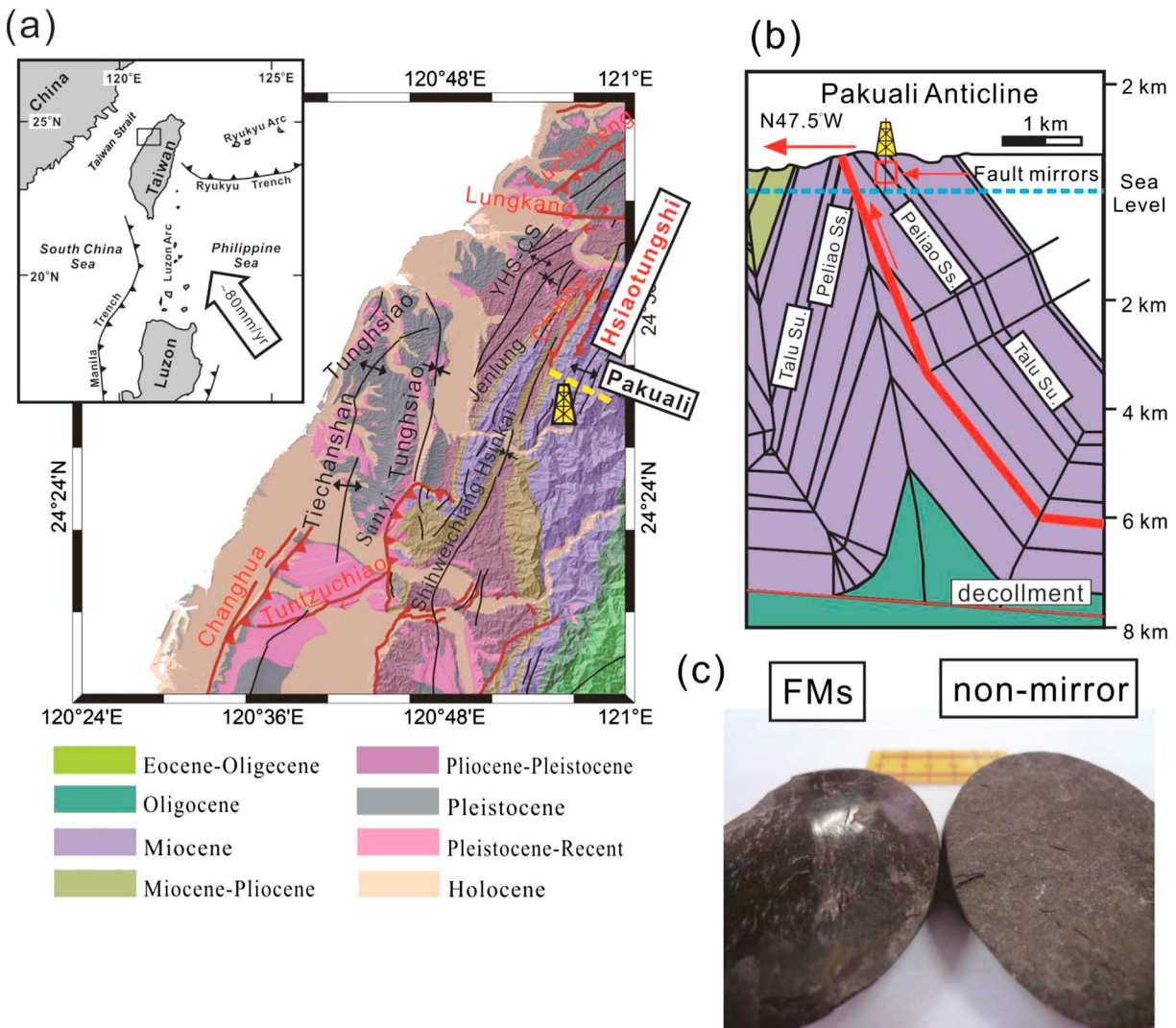


Figure 1. (a) Shaded-relief geological map combing time-stratigraphic units showing the fold-and-thrust belt of the Miaoli-Hsinchu area, and the Hsiaotungshi active reverse fault bounded the eastern side of the Miaoli-Hsinchu area. The drill site is located in the hanging wall of the Hsiaotungshi active reverse fault (modified from Chinese Petroleum Corporation, 1974 and 1978). The inset box shows a schematic drawing of tectonic of Taiwan. (b) Cross section of the drilling site showing structural interpretation through the eastern part of the Miaoli-Hsinchu area (after Namson [1981]). The Hsiaotungshi fault zone plotted as the heavy red line, and the black line is the boundary of lithological formations. (c) Photograph of highly reflective surface recognized as FM fault surface and nonmirror surface.

2. Geological Setting

The mountainous island of Taiwan is developed by arc-continent collision in which the Philippine Sea plate moves northwestward at an average velocity of ~80 mm/yr with respect to Eurasian continent [Yu *et al.*, 1997] (Figure 1a inset). Approximately a third of this convergence is consumed within the complex western Taiwan fold-and-thrust belt where recent large earthquakes such as the 1999 Chi-Chi $M_w = 7.6$ and 1935 Hsinchu-Miaoli MGR = 7.1 earthquakes occurred [Le Béon *et al.* 2014; Shyu *et al.*, 2005] (Figure 1a). The Hsiaotungshi reverse fault lies within the east limb of the Pakuali anticline, which activated the 1935 Hsinchu-Miaoli earthquake (Figure 1b). The host rock of the Hsiaotungshi reverse fault consists of well-consolidated Oligocene-Miocene sedimentary sequences up to 4500 m thick (Figures 1a and 1b).

The drilling site was located in the east of the Hsiaotungshi fault system, and the cores were recovered from the hanging wall damage zone in the shallow marine Talu Shale (Miocene) and Peliao Sandstone (early Miocene) at depths of 500 to 600 m (Figure 1b). Talu Shale mainly consists of very thin bedded shale with evenly dispersed medium to fine-grained mica (Figure 1c). Peliao Sandstone is primarily composed of muddy

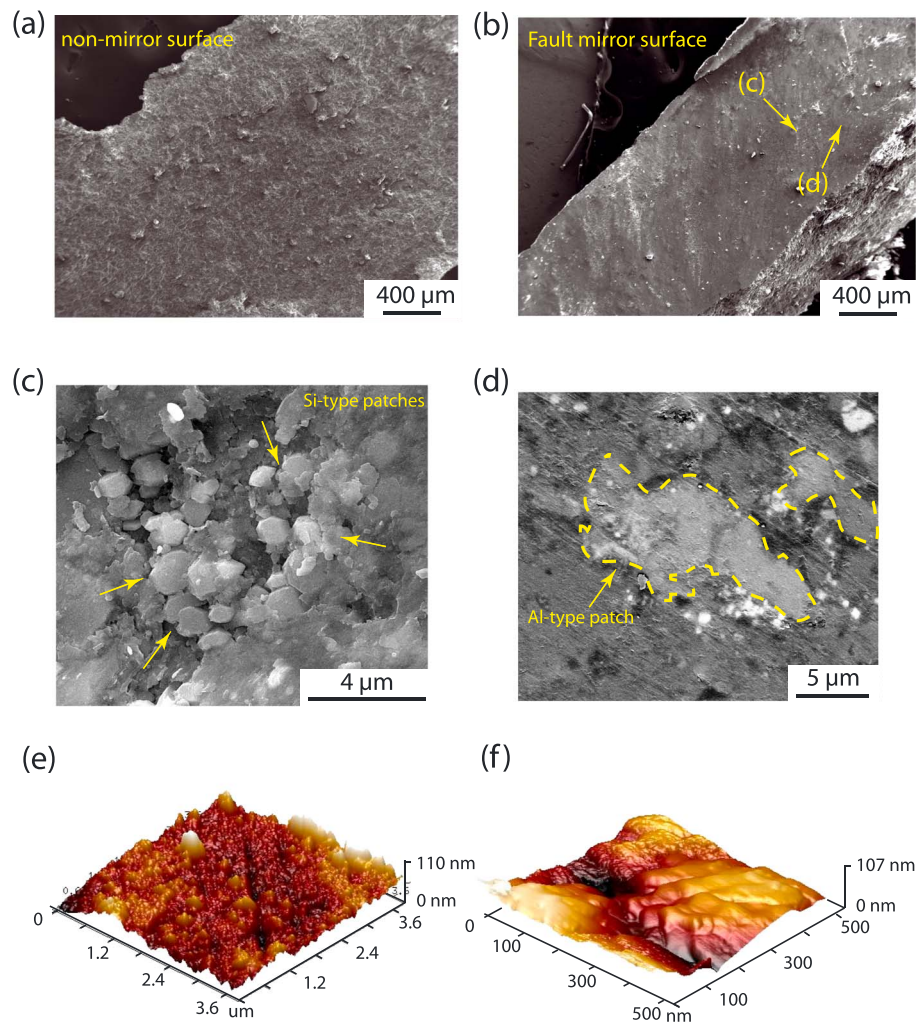


Figure 2. Representative microstructures of both nonmirror surface and FMs. (a) Field emission scanning electron microscopy (FE-SEM) image showing roughness and coarse grains on the nonmirror surface. (b) FE-SEM image showing ultrasmooth surface of a FM. (c) Matrix of FMs consists of roughly hexagonal aggregates ranged from <1 to $2\ \mu\text{m}$ in size (indicated with yellow arrows) separated by micrometer-scale, angular pores. (d) Al-type patches are anhedral (indicated with yellow dashed line) and heterogeneously distributed. (e) Atomic force microscopy (AFM) morphology scans of the Si-type patches. Darker colors represent lower regions; brighter colors represent higher regions. The Si-type patches from top three-dimensional view are very flat except for several scratches and few prominent grains and grooves. (f) AFM morphology scans of the Al-type patches from three-dimensional view are very flat and showing wavy morphology.

sandstone with a few clean sandstone beds and shale strata. These formations show well-preserved sedimentary features such as bedding-parallel orientation of platy minerals and bioturbation structures, and no diagenetic amorphous materials are reported [Namson, 1981; Ho, 1994]. It is interesting that several fault or joint surfaces, which are generally bedding-parallel, were found. In particular, some surfaces are rough and nonreflective, whereas others are highly reflective, the so-called fault mirrors (FMs) (Figure 1c). The FMs, in general, are widely distributed stratigraphically and were found on many cores, which display well-polished fault surfaces characterized by high visible-light reflectivity with vitreous luster (Figure 1c).

3. Material and Methods

We performed extensive characterization of these FMs and their context, including (1) observed microstructures and composition of both nonmirror surfaces (planar fracture surface; bedding plane of host rocks) and FMs from surface view and cross-section view (petrographic section perpendicular to the FMs) with field emission scanning

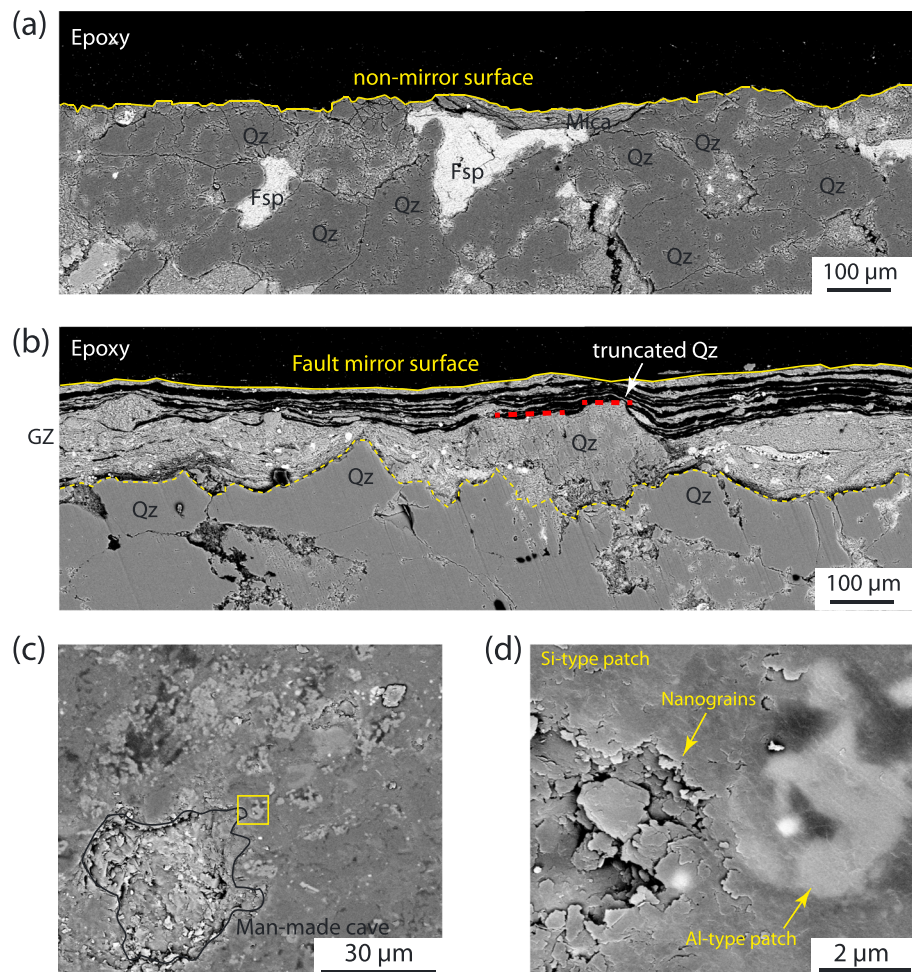


Figure 3. Representative microstructures in cross section of both nonmirror surface and FMs. (a) Backscattered electron (BSE) image in cross section showing roughness and coarse grains along the nonmirror surface. (b) BSE image in cross section showing ultrasmooth surface along FMs. Truncated quartz grains along FMs marked with red line. (c) BSE image on tilted FMs. The cave made by a pin to expose underlying material was marked with black line. The yellow rectangle was enlarged in 3-D. (d) BSE image illustrating a few dozens of nanometers thick amorphous silica on FMs. The out-of-focus Al-type patch resulted from the tilted analyzed surfaces.

electron microscopy equipped with an energy dispersive spectrometer at 10 kV (FESEM/EDX), (2) measured roughness and morphology of FMs on nanoscales with atomic force microscopy (AFM), (3) recognized crystallinity of analyzed materials from FMs with transmission electron microscopy (TEM), (4) detected the water content of FMs with micro-Raman spectroscopy, and in particular (5) determined mineral assemblages of host rock and gouge zone with and without FMs by in situ synchrotron X-ray diffraction analyses (see method and condition of in situ synchrotron X-ray diffraction (XRD) in the supporting information) (Figures 2, 3, and 4). The FMs appear as a hard shield on the fault surface coating thin gouge layers below. We gently separated hard films (FMs) from gouge zone and directly analyzed FMs; however, it seems that part of contribution of the XRD intensity was derived from gouge just next to FMs in the in situ synchrotron XRD analyses (Figure 4).

4. Results

The nonmirror surfaces observed in hand specimen commonly contain a number of tiny visible platy mica and fine sand grains of quartz and feldspar (Figure 1c). Even though the nonmirror surfaces look relatively planar at the centimeter scale, the irregularities observed derive from the breakup of grain boundary, roughly parallel or subparallel to the orientation of platy mica. In contrast, the FMs observed in hand specimen overlie

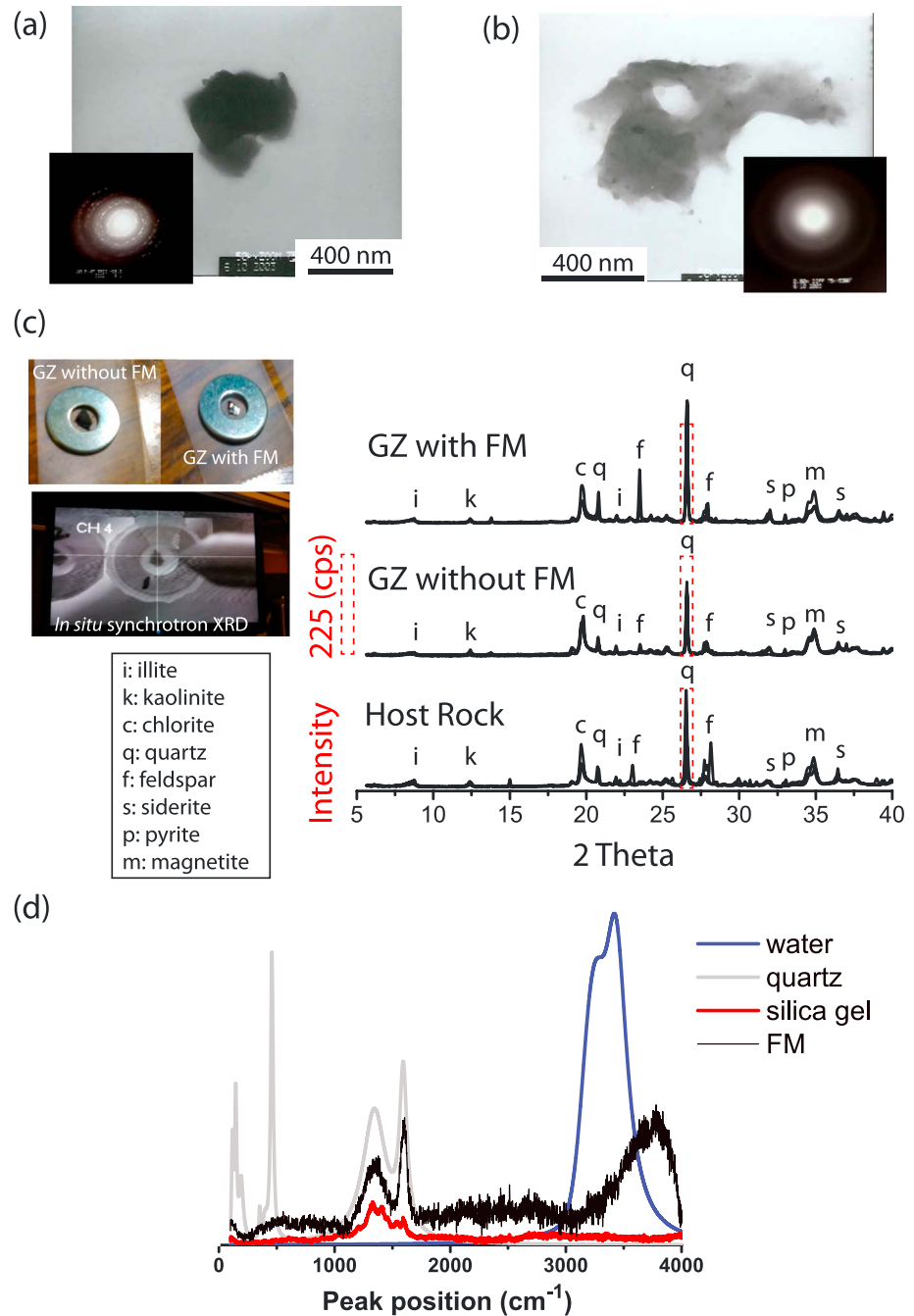


Figure 4. Characterization of mineral assemblages of both host rocks and FMs. (a) Transmission electron microscopy (TEM) images of the grains collected from the Si-type patches. Selected area electron diffraction pattern (SAED) of the Si-type patches showing some nanograins and glassy matrix. (b) TEM images of the grains collected from the Al-type patches. SAED of the Al-type patches showing no light spots indicating only glassy matrix in this grain. (c) Samples for the analysis of in situ synchrotron XRD analysis are shown in the top left side. The mineral assemblages of host rock are very similar to that of the gouge zone either covered by FMs or without FMs. Comparing the abundance of quartz (red dashed rectangle), the gouge zone covered with fault mirrors is relatively enriched in quartz, which suggests that quartz is the dominant component on fault mirrors. cps, counts per second. (d) Spectra of micro-Raman analyses showing that silica gel and water are presented on FMs.

Table 1. Average Cation Compositions of Minerals on FMs Determined by FESEM-EDS (Unit in wt %)

Phases	Ferrous Minerals	Carbonaceous Materials	Clay Minerals	Si-type Patches	Al-type Patches
n	24	9	16	20	34
Mg	3.7	0	1.7	0	1.9
Si	5.9	7.6	50.0	90.3	50.8
Ca	2.6	0	0	0	0
Mn	4.5	0	0	0	0
Fe	47.2	2.3	4.2	4.3	12.7
Al	0.8	5	28.5	4.3	19.1
K	0	0.2	15.0	0.5	15.5
Ti	0	1.2	0.9	0	0
C	35.3	83.7	0	0	0
Na	0	0	0	0.3	0
S	0	0	0	0.3	0
Sum	100	100	100	100	100

thin generally bedding-parallel ($\sim 10^{-3}$ to 10^{-2} m) gouge layers [cf. *Hung and Yang, 1991*] and commonly appears as very shiny and hard, sometimes showing corrugations, undulations, and fine grooves (Figure 1c).

At the micrometer scale of surface view, the nonmirror surface shows obvious roughness derived from micrometers to millimeters quartz clasts and feldspar grains (Figure 2a). In contrast, FMs appear to be ultrasmooth with no clear grain boundaries (Figure 2b). FMs are dominantly composed of nanograins and anhedral amorphous patches (Figures 2c and 2d), with very few ferrous minerals and carbonaceous materials (Table 1; supporting information). Sometimes the matrix is composed of tens of micrometer-sized angular to rounded quartz clasts. The chemical composition of the siliceous materials in the matrix can be divided into two types: the silica-rich patches (Si-type patches) that are the main domain of FMs (Figure 2c) and the alumina-rich patches (Al-type patches) (Figure 2d and Table 1). The Si-type patches consist of roughly hexagonal aggregates that range from <1 to $2\ \mu\text{m}$ in size separated by micrometer scale with angular pores and are randomly or weakly oriented (arrowheads in Figure 2c). The Al-type patches commonly appear to be anhedral and are heterogeneously distributed on the FMs (Figure 2d).

Imaging mode atomic force microscopy (AFM) using a sharp-tip probe shows two distinctive domains for the FMs matrix. Most of the Si-type patches commonly are aggregates with diameters of tens to hundreds of nanometers with small-scale striations or grooves (Figure 2e), whereas the Al-type patches display wavy undulations without obvious grain boundary (Figure 2f). At the nanoscale of surface view, the roughness of FMs, computed by root-mean-square (RMS) of roughness [*Power and Tullis, 1991*], is ~ 15 nm and 19 nm, respectively, for matrix and melt patches under the wavelength of 550 nm (see measurements of AFM in the supporting information). Therefore, the RMS of FMs is smaller than 100 nm under visible light and the glossy surfaces must obey the Rayleigh roughness criterion [*Beckmann and Spizzichino, 1963; Siman-Tov et al., 2013*].

At the micrometer scales in cross section view, irregularity is observed along the nonmirror surface (Figure 3a), which is derived from the angular shapes of grains and platy minerals. The orientation of platy minerals such as mica underlying and parallel to the nonmirror surface suggests that the nonmirror surface is parallel to bedding. In contrast, in the FM case a thin gouge zone ranging from tens to hundreds of micrometers in thickness usually underlies the FMs (Figure 3b). With respect to the roughness of FMs, the boundary between gouge zone and host rock is irregular (Figure 3b), and several open fractures filled with epoxy parallel to subparallel the boundary separate the thin zone of aligned clay minerals (dark area of the gouge zone in Figure 3b). In particular, the quartz clast along FMs appears to be truncated suggesting the strong shear strain localization during the formation of FMs (the white arrow in Figure 3b). The gouge zone is relatively enriched in clay minerals and contains fewer angular to rounded clasts of quartz and feldspar smaller than the surrounding host rock. A stacked sheet of overlapping clay minerals and micrometer-sized quartz grains are observed along the FMs trace, whereas the Si-type patches are not observed along FMs. This was presumably resulted from mechanical erosion during sample preparation. In order to understand the spatial occurrence of the Si-type patches on FMs, we carved the FMs with a pin and observed the man-made cliff on a tilted sample stage of 30° with scanning electron microscopy (SEM) (Figure 3c). It seems that the Si-type patches are dominantly composed of nanograins that were smeared on the FMs.

TEM analyses suggest that (1) the Si-type patches are primarily composed of both well-structured quartz nanograins and amorphous materials and (2) the Al-type patches do not have crystal lattice and are amorphous (Figures 4a and 4b). The results of in situ synchrotron X-ray analysis show that the mineral assemblages of host rock, gouge zone with and without FMs are composed mainly of quartz, feldspar, illite, chlorite, kaolinite, siderite, magnetite, and pyrite (Figure 4c). It is notable that the intensity of quartz peak in the sample of gouge zone with FMs is the highest among the analyzed samples. The synchrotron XRD results suggest that the quartz is more abundant in FMs and is also in good agreement with our observation by FESEM/EDX (Figure 2b). Both the scarceness of the amorphous patches and relatively low intensity of the amorphous peak contribute to the difficulty of their being recognized in the XRD patterns. The 100–4000 cm^{-1} region of Raman spectrum, which includes the first-order bands of silica gel, suggests that the Si-type patches on FMs are gel origin amorphous patches (Figure 4d), based on comparison with the spectra of the commercial standards including quartz, silica gel, and water. In addition, it seems that the Si-type amorphous patches are hydrous on the basis of the similarity of the region from 3000 cm^{-1} to 4000 cm^{-1} of Raman spectra between FMs and water, although the main peak location of the Si-type patches is different from the one for water, presumably resulting from the different types of hydroxide. In general, the mineralogy of FMs is identical to the host rock, except the presence of the Si-type patches that include amorphous materials and micrometer-sized quartz grains, and the presence of amorphous Al-type patches.

5. Discussion and Conclusion

The occurrence of mirror fault surfaces, cutting parallel to a regional fault surface, within fault gouges, suggests that they are fault related and thus termed FMs (Figure 1). Rock friction experiments on carbonate rocks indicate and gouge that mirror-like surfaces can be developed at both subseismic rates (0.1–10 $\mu\text{m/s}$) [Verberne *et al.*, 2013, 2014] and seismic rates (0.07–0.1 m/s) [Fondriest *et al.*, 2013; Siman-Tov *et al.*, 2015]. In addition, multiple mechanisms for the formation of glossy surfaces, such as reorientation of grains (Power and Tullis), alignment and preferred orientation of clay minerals [Will and Wilson 1989; Laurich *et al.*, 2014], development of gels [Kirkpatrick *et al.*, 2013], and formation of nanoparticles [De Paola, 2013], have been proposed. It seems that mirror-like surfaces are not necessarily formed at fast fault slip. However, the presence of truncated quartz clasts along our FMs was presumably associated to strong shear strain localization (Figure 3b), which suggests they were formed at fast coseismic slip rates, as was previously documented in both experimentally deformed and natural dolomitic gouges [Fondriest *et al.*, 2013, 2015]. Therefore, the FMs in this study are reminiscent of tribofilms obtained in industrial and rock friction experiments in which sintering has occurred during high velocity slip (Figure 3d) [Adachi and Kato, 2000; Hirose *et al.*, 2012].

The studied FMs are hard glossy surfaces that separate gouge zones and are mainly composed of the Si-type and the Al-type amorphous patches (Figure 3d). On the basis of our results, observations that Si-type patches are hydrous (Figure 4d) and amorphous (Figures 4a and 4c), we interpret them as hydrated amorphous silica gel. Multiple natural origins of hydrated amorphous silica gel have been suggested: (1) by comminution and hydrolization during cataclasis [Di Toro *et al.*, 2004]; (2) by precipitation of a hydrothermal fluid [Power and Tullis, 1989]; and (3) by on-fault reactions concurrent with slip [Herrington and Wilkinson, 1993], and thus, the determination of the origin of frictional silica gel products in faults remains challenging. Four lines of evidence suggest that the silica gel in the studied FMs was generated by the cataclastic mechanism: (1) the deformation structures on FMs (slickensides and aligned overlapping clay minerals in thin section) are in kinematic agreement with fault slip; (2) because silica gel must form from hydration during frictional wear [Di Toro *et al.*, 2011], the silica gel and micrometer-sized quartz mixing within the FMs suggest the FMs formed in the presence of fluids during cataclastic deformation; (3) the mineralogy of FMs is identical to that of the host rock with no evidence for the incoming of foreign fluids; and (4) there are no known magmatic rocks, hydrothermal deposits, and biogenic opal associated with the rock units in the area, and silica gel seems unlikely to be derived from magmatic and biogenic origins [Ho, 1994]. Finally, the hydrated amorphous silica gel and micrometer-sized quartz grains documented here most closely resemble the products of the rock friction experiments, suggesting a cataclastic origin.

Rock friction experiments demonstrated that silica gel forms in silica-rich rocks at moderate to high slip rates by frictional wear at ambient air humidity [Hayashi and Tsutsumi, 2010; Nakamura *et al.*, 2012]. Silica must amorphize and hydrate to form gel, and cataclasis during the rock friction experiments has been suggested

to facilitate hydrolization and amorphization by generating reactive quartz surfaces for silica gel formation [Di Toro et al., 2011; Di Toro et al., 2004; Goldsby and Tullis, 2002]. Silica amorphization is also observed under static pressure [25–35 GPa; Hemley et al., 1988] and at a variety of applied stresses, bulk displacement rates, and temperatures [Yund et al., 1990; Pec et al., 2012]. Given the range of slip rates, and conditions at which it may be formed, the specific conditions for the formation of silica gel of our observed FMs are still uncertain, even if hydrated amorphous silica gel were shown to be formed frictionally. However, the shear-weakening rheology documented by the silica gel forming experiments indicate that regardless of the mode of formation, silica gel on fault surfaces are likely to have significant slip-weakening effects [Goldsby and Tullis, 2002; Di Toro et al., 2004]. Further microphysical models constrained by rock deformation experiments on silica gel are required to decipher plausible fault slip behaviors on the studied FMs.

There are two possible origins for the Al-type amorphous materials: either extremely fine comminution of crystalline particles or melting. Compared with the observation of extremely comminution by Yund et al. [1990], we strongly favor the second interpretation for the reasons that are (1) the amorphous patches have anhedral boundaries and there appears to be sharp boundary between amorphous patches and silica gel, instead of being continuum by extreme comminution, (2) the amorphous patches seem somewhat nonporous as indicated by extreme comminution, and (3) the amorphous patches are rare (less than a few percent) and heterogeneously distributed on FMs, instead of being abundant (up to 50 %) in the matrix on localized “Y” surface defined by Logan et al. [1979]. The chemical analysis using the SEM-EDX reveals that the composition of the Al-type amorphous patches is similar to those of the mixture of clay minerals (e.g., illite, chlorite, and kaolinite). The AFM image of the Al-type patches shows wavy undulations, suggesting a melt origin (Figure 2f). Besides which, the previous study shows no clear evidence of amorphous materials in the studied formation (Talu Shale and Peliao sandstone) (Figure 2b) [Ho, 1994]. Consequently, it seems that the Al-type amorphous patches on FMs are the product of frictional melt presumably derived from surrounding clay minerals.

Integrated observation of natural and simulated fault products suggests that frictional melting of clayey gouge can occur during seismic slip [Kuo et al., 2009; Han et al., 2014]. Han et al. [2014] observed that melt patches were generated locally in the marginal area of the gouge zone and suggested flash heating [e.g., Rice, 2006] as the mechanism forming melt patches. Flash heating and weakening has also been demonstrated to explain large reduction of shear strength on silicate-hosted rocks [Goldsby and Tullis, 2011]. In particular, flash heating occurring at very short displacement during seismic slip is expected to dominate the strength of the fault for relatively small slip in small earthquakes and in the initial slip stages of large earthquakes [Goldsby and Tullis, 2011; Han et al., 2014]. For the cases of frictional melting of fault gouge, continued slip (or large displacement) may increase bulk and flash temperature within gouge zone, leading to the connection of melt patches and, consequently, formation of a melt layer [Han et al., 2014]. Given the evidences of (1) heterogeneous distribution of the melt patches on FMs (Figures 2d and 3d), (2) no obvious vesicles on FMs or within the gouge zone (Figures 2b and 3b), and (3) no apparent mineral anomaly (Figure 4c), it suggests that the melt patches on observed FMs were generated at high temperature of asperities in short slips rather than being produced at high bulk temperature of fault zones with large slip, as was documented in the case in the nearby Chi-Chi earthquake $M_w = 7.6$ [e.g., $> 900^\circ\text{C}$; Kuo et al., 2011].

We link those main features of FMs with associated bedding-parallel gouge layers from the hanging wall damage zone of the Hsiaotungshi active reverse system: they are a smooth, glossy film (Figure 1c) that is composed of silica gel, micrometer-sized quartz, and melt patches resulted from small fast slip (Figures 2 and 3). On the basis of their stratigraphic and structural setting [Namson, 1981], we suggest that these small faults were active shallower than ~ 4 km. We could not constrain the displacement of observed FMs since the core is only a pin point along the whole fault surfaces. Similar bedding-parallel approximately millimeter-scale gouge zones are observed to extend for more than 5 m in outcrops of the adjacent Chuhuangkeng anticline [Hung and Yang, 1991]; however, we are unable to observe the size of the FM patches within the gouge layers. It seems that the entire bedding fault slips in single earthquake, but FMs are just a development at local patches of currently unknown size in any earthquake. We simply assume that displacement of few millimeters to centimeters occurred for generating melt patches as suggested by rock friction experiments [Goldsby and Tullis, 2011]. The estimated slip from the observation of FMs is also in good agreement with our field observation by the fact that accommodated slip along FMs, parallel to bedding surfaces which are the limbs of an anticline fold and found no clear evidence of mesoscale fold disruption, should be small [Hung and Yang, 1991]. Seismological

scaling relationships indicate that these fault rocks could be the product of small earthquakes ($< M0$) with few millimeters of slip and slip durations of tens to hundreds of milliseconds [Wells and Coppersmith, 1994; Boettcher et al., 2009; Kwiatak et al., 2011]. It seems likely that the occurrence of the FMs represent a fossil of small earthquakes as the consequence of accommodated coseismic faulting and folding, in particular coseismic flexural slip, or aftershock deformation in the active western Taiwan fold-and-thrust belt [Le Béon et al., 2014; Shyu et al., 2005].

We conclude that (1) FMs were characterized as an ultrasmooth surface composed of silica gel, micrometer-sized quartz grains, and melt patches; (2) FMs were formed at fast fault slips; (3) silica gel was generated by a cataclastic process; (4) the melt patches were produced by flash heating at asperities; and (5) the occurrence of FMs in our case represent fossil of small earthquakes as the consequence of accommodated coseismic faulting and folding or aftershock deformation in the active western Taiwan fold-and-thrust belt. We envision that the presence of FMs can be a widespread phenomenon along natural faults [Power and Tullis, 1989; Fondriest et al., 2013; Siman-Tov et al., 2013; Kuo et al., 2014; Evans et al., 2014]. Since our results indicate that FMs may represent a fossil of ancient small earthquakes, the occurrence of FMs can be used to assess seismic hazard in tectonically active regions, especially those with incomplete earthquake catalogues.

Acknowledgments

We thank the reviewer De Paola, two anonymous reviewers, and Editor Andrew V. Newman for their positive and constructive comments. We also thank Jiann-Neng Fang, Dr. Yu-Ting Kuo, and Hsiu-Ching Hsiao for their laboratory support. We thank Hwo-Shuenn Sheu for the technical support for our in situ synchrotron XRD analysis work. All microstructural observation used in this study are available by contacting the corresponding author L.-W. Kuo (liweikuo@ncu.edu.tw). This work was supported by Ministry of Science and Technology (MOST 104-2116-M-008-026 to L.-W. Kuo and MOST 103-2116-M-002-014 to S.-R. Song), National Taiwan University (104R104051 to J. Suppe), and National Natural Science Foundation of China (41330211).

References

- Adachi, K., and K. Kato (2000), Formation of smooth wear surfaces on alumina ceramics by embedding and tribo-sintering of fine wear particles, *Wear*, *245*, 84–91, doi:10.1016/S0043-1648(00)00468-3.
- Allen, J. L. (2005), A multi-kilometer pseudotachylyte system as an exhumed record of earthquake rupture geometry at hypocentral depth (Colorado, USA), *Tectonophysics*, *402*, 37–54.
- Beckmann, P., and A. Spizzichino (1963), *The Scattering of Electromagnetic Waves From Rough Surfaces*, Int. Ser. Monogr. Electromagn. Waves, vol. 4, 503 pp., Pergamon Press, Oxford, U. K.
- Boettcher, M. S., A. McGarr, and M. Johnston (2009), Extension of Gutenberg-Richter distribution to $M_W - 1.3$, no lower limit in sight, *Geophys. Res. Lett.*, *36*, L10307, doi:10.1029/2009GL038080.
- Camacho, A., R. H. Vernon, and J. D. Fitz Gerald (1995), Large volumes of anhydrous pseudotachylyte in the Woodroffe Thrust, eastern Musgrave Ranges, Australia, *J. Struct. Geol.*, *17*, 371–383.
- Collettini, C., C. Viti, T. Tesi, and S. Mollo (2013), Thermal decomposition along natural carbonate faults during earthquakes, *Geology*, *41*, 927–930.
- De Paola, N. (2013), Nano-powder coating coating can make fault surfaces smooth and shiny: Implications for fault mechanics?, *Geology*, *41*, 719–720, doi:10.1130/focus062013.1.
- Di Toro, G., and G. Pennacchioni (2005), Fault plane processes and mesoscopic structure of a strong-type seismogenic fault in tonalites (Adamello batholith, Southern Alps), *Tectonophysics*, *402*, 54–79.
- Di Toro, G., D. L. Goldsby, and T. E. Tullis (2004), Friction falls towards zero in quartz rock as slip velocity approaches seismic rates, *Nature*, *427*, 436–439.
- Di Toro, G., T. Hirose, S. Nielsen, G. Pennacchioni, and T. Shimamoto (2006), Natural and experimental evidence of melt lubrication of faults during earthquakes, *Science*, *311*, 647–649.
- Di Toro, G., G. Pennacchioni, S. Nielsen, and F. Eiichi (2009), Pseudotachylytes and earthquake source mechanics, in *Fault-zone Properties and Earthquake Rupture Dynamics*, Int. Geophys. Ser., vol. 94, edited by E. Fukuyama, pp. 87–133, Elsevier, Amsterdam.
- Di Toro, G., R. Han, T. Hirose, N. De Paola, S. Nielsen, K. Mizoguchi, F. Ferri, M. Cocco, and T. Shimamoto (2011), Fault lubrication during earthquakes, *Nature*, *471*, 494–498, doi:10.1038/nature09838.
- Evans, J. P., M. R. Prante, S. U. Janekke, A. K. Ault, and D. Newell (2014), Hot faults: Iridescent slip surfaces with metallic luster document high-temperature ancient seismicity in the Wasatch fault zone, Utah, USA, *Geology*, *42*(7), 623–626.
- Fondriest, M., S. A. F. Smith, T. Candela, S. Nielsen, K. Mair, and G. Di Toro (2013), Mirror-like faults and power dissipation during earthquakes, *Geology*, doi:10.1130/G34641.1.
- Fondriest, M., S. Atretusini, G. Di Toro, and S. A. F. Smith (2015), Fracturing and rock pulverization along an exhumed seismogenic fault zone in dolostones: The Foiana Fault Zone (Southern Alps, Italy), *Tectonophysics*, *654*, 56–74.
- Goldsby, D. L., and T. E. Tullis (2002), Low frictional strength of quartz rocks at subseismic slip rates, *Geophys. Res. Lett.*, *29*(17), 1844, doi:10.1029/2002GL015240.
- Goldsby, D. L., and T. E. Tullis (2011), Flash heating leads to low frictional strength of crustal rocks at earthquake slip rates, *Science*, *334*, 216–218.
- Han, R., T. Shimamoto, T. Hirose, J.-H. Ree, and J. I. Ando (2007), Ultralow friction of carbonate faults caused by thermal decomposition, *Science*, *316*(5826), 878–881.
- Han, R., T. Hirose, G. Y. Jeong, J.-i. Ando, and H. Mukoyoshi (2014), Frictional melting of clayey gouge during seismic fault slip: Experimental observation and implications, *Geophys. Res. Lett.*, *41*, 5457–5466, doi:10.1002/2014GL061246.
- Hayashi, N., and A. Tsutsumi (2010), Deformation textures and mechanical behavior of a hydrated amorphous silica formed along an experimentally produced fault in chert, *Geophys. Res. Lett.*, *37*, L12305, doi:10.1029/2010GL042943.
- Hemley, R. J., A. P. Jephcoat, H. K. Mao, L. C. Ming, and M. H. Manghnani (1988), Pressure-induced amorphization of crystalline silica, *Nature*, *334*, 52–54, doi:10.1038/334052a0.
- Herrington, R. J., and J. J. Wilkinson (1993), Colloidal gold and silica in mesothermal vein systems, *Geology*, *21*, 539–542.
- Hirose, T., K. Mizoguchi, and T. Shimamoto (2012), Wear processes in rocks at slow to high slip rates, *J. Struct. Geol.*, *38*, 102–116, doi:10.1016/j.jsg.2011.12.007.
- Ho, H. C. (1994), Explanatory text of the geological map of Taiwan, Scale 1:50,000, sheet 12, Miaoli, *Central Geological Survey, The Ministry of Economic Affairs*, p. 69.
- Hung, J. H., and C. N. Yang (1991), Mesoscale deformation mechanisms in the Chuhuangkeng anticline, Miaoli, Taiwan, *Proc. Geol. Soc. China*, *34*, 17–42.

- Kirkpatrick, J. D., C. D. Rowe, J. C. White, and E. E. Brodsky (2013), Silica gel formation during fault slip: Evidence from the rock record, *Geology*, *41*(9), 1015–1018.
- Kuo, L.-W., S.-R. Song, E.-C. Yeh, and H.-F. Chen (2009), Clay mineral anomalies in the fault zone of the Chelungpu Fault, Taiwan, and their implications, *Geophys. Res. Lett.*, *36*, L18306, doi:10.1029/2009GL039269.
- Kuo, L.-W., S.-R. Song, L. Huang, E.-C. Yeh, and H.-F. Chen (2011), Temperature estimates of coseismic heating in clay-rich fault gouges, the Chelungpu fault zones, Taiwan, *Tectonophysics*, *502*, 315–327.
- Kuo, L.-W., et al. (2014), Gouge graphitization and dynamic fault weakening during the 2008 Mw 7.9 Wenchuan earthquake, *Geology*, *42*, 47–50.
- Kwiatek, G., K. Plenkers, and G. Dresen (2011), Source parameters of picoseismicity recorded at Mponeng Deep gold mine, South Africa: Implications for scaling relations, *Bull. Seismol. Soc. Am.*, *101*, 2592–2608, doi:10.1785/0120110094.
- Laurich, B., J. L. Urai, G. Desbois, C. Vollmer, and C. Nussbaum (2014), Microstructural evolution of an incipient fault zone in Opalinus Clay: Insights from an optical and electron microscopic study of ion-beam polished samples from the Main Fault in the Mt-Terri Underground Research Laboratory, *J. Struct. Geol.*, *67*, 107–128, doi:10.1016/j.jsg.2014.07.014.
- Le Béon, M., J. Suppe, M. J. Jaiswal, Y. G. Chen, and M. E. Ustaszewski (2014), Deciphering cumulative fault slip vectors from fold scarps: Relationships between long-term and coseismic deformations in central Western Taiwan, *J. Geophys. Res. Solid Earth*, *119*, 5943–5978, doi:10.1002/2013JB010794.
- Logan, J. M., M. Friedman, N. Hoggs, C. Dengo, and T. Shimamoto (1979), Experimental studies of simulated gouge and their application to studies of natural fault zones, in *Proceedings of Conference VIII on Analysis of Actual Fault Zones in Bedrock, U.S. Geol. Surv. Open File Rep.*, 79–1239.
- Nakamura, Y., J. Muto, H. Nagahama, I. Shimizu, and T. Miura (2012), Amorphization of quartz by friction: Implication to silica-gel lubrication of fault surfaces, *Geophys. Res. Lett.*, *39*, L21303, doi:10.1029/2012GL053228.
- Namson, J. (1981), Structure of the Western Foothills Belt, Miaoli-1094 Hsinchu area, Taiwan; I, Southern part, *Pet. Geol. Taiwan*, *18*, 31–51.
- Niemeijer, A., G. Di Toro, W. A. Griffith, A. Bistacchi, S. A. F. Smith, and S. Nielsen (2012), Inferring earthquake physics and chemistry using an integrated field and laboratory approach, *J. Struct. Geol.*, *39*, 2–36, doi:10.1016/j.jsg.2012.02.018.
- Pec, M., H. Stünitz, R. Heilbronner, M. Drury, and C. de Capitani (2012), Origin of pseudotachylytes in slow creep experiments, *Earth Planet. Sci. Lett.*, *355–356*, 299–310, doi:10.1016/j.epsl.2012.09.004.
- Polissar, P. J., M. H. Savage, and E. E. Brodsky (2011), Extractable organic material in fault zones as a tool to investigate frictional stress, *Earth Planet. Sci. Lett.*, *311*, 439–447, doi:10.1016/j.epsl.2011.09.004.
- Power, W. L., and T. E. Tullis (1989), The relationship between slickenside surfaces in fine-grained quartz and the seismic cycle, *J. Struct. Geol.*, *11*, 879–893, doi:10.1016/0191-8141(89)90105-3.
- Power, W. L., and T. E. Tullis (1991), Euclidean and fractal models for the description of rock surface roughness, *J. Geophys. Res.*, *96*, 415–424, doi:10.1029/90JB02107.
- Rice, J. R. (2006), Heating and weakening of faults during earthquake slip, *J. Geophys. Res.*, *111*, B05311, doi:10.1029/2005JB004006.
- Rowe, C. D., A. Fagereng, J. A. Miller, and B. Mapani (2012a), Signature of coseismic decarbonation in dolomitic fault rocks of the Naukluft thrust, Namibia, *Earth Planet. Sci. Lett.*, *333–334*, 200–210.
- Rowe, C. D., J. D. Kirkpatrick, and E. E. Brodsky (2012b), Fault rock injections record paleo-earthquakes, *Earth Planet. Sci. Lett.*, *335–336*, 154–166.
- Savage, H. M., P. J. Polissar, R. Sheppard, C. D. Rowe, and E. E. Brodsky (2014), Biomarkers heat up during earthquakes: New evidence of seismic slip in the rock record, *Geology*, *42*(2), 99–102.
- Shyu, J. B. H., K. Sieh, Y. G. Chen, and C. S. Liu (2005), Neotectonic architecture of Taiwan and its implications for future large earthquakes, *J. Geophys. Res.*, *110*, B08402, doi:10.1029/2004JB003251.
- Sibson, R. H. (1975), Generation of pseudotachylyte by ancient seismic faulting, *Geophys. J. R. Astron. Soc.*, *43*(3), 775–794.
- Siman-Tov, S., E. Aharonov, A. Sagy, and S. Emmanuel (2013), Nanograins form carbonate fault mirrors, *Geology*, *41*(6), 703–706.
- Siman-Tov, S., E. Aharonov, Y. Boneh, and Z. Reches (2015), Fault mirrors along carbonate faults: Formation and destruction during shear experiments, *Earth Planet. Sci. Lett.*, *430*, 367–376.
- Smith, S. A. F., G. Di Toro, S. Kim, J.-H. Ree, S. Nielsen, A. Billi, and R. Spiess (2013), Coseismic recrystallization during shallow earthquake slip, *Geology*, *41*, 63–66, doi:10.1130/G33588.1.
- Spray, J. G. (1987), Artificial generation of pseudotachylyte using friction welding apparatus: Simulation of melting on a fault plane, *J. Struct. Geol.*, *9*(1), 49–60.
- Swanson, M. T. (1992), Fault structure, wear mechanisms and rupture processes in pseudotachylyte generation, *Tectonophysics*, *204*, 223–242.
- Tsutsumi, A., and T. Shimamoto (1997), High-velocity frictional properties of gabbro, *Geophys. Res. Lett.*, *24*(6), 699–702, doi:10.1029/97GL00503.
- Verberne, B. A., J. H. P. de Bresser, A. R. Niemeijer, C. J. Spiers, D. A. M. de Winter, and O. Plümpner (2013), Nanocrystalline slip zones in calcite fault gouge show intense crystallographic preferred orientation: Crystal plasticity at sub-seismic slip rates at 18–150°C, *Geology*, *41*, 863–866.
- Verberne, B. A., O. Plümpner, D. A. M. de Winter, and C. J. Spiers (2014), Superplastic nanofibrous slip zones control seismogenic fault friction, *Science*, *346*(6215), 1342–1344.
- Wells, D. L., and K. J. Coppersmith (1994), New empirical relationships among magnitude, rupture length, rupture width, rupture area, and surface displacement, *Seismol. Soc. Am., Bull.*, *4*, 974–1002.
- Will, T. M., and C. J. Wilson (1989), Experimentally produced slickenside lineations in pyrophyllitic clay, *J. Struct. Geol.*, *11*, 657–667.
- Yu, S. B., H. Y. Chen, and L. C. Kuo (1997), Velocity field of GPS stations in the Taiwan area, *Tectonophysics*, *274*(1–3), 41–58.
- Yund, R. A., M. L. Blanpied, T. E. Tullis, and J. D. Weeks (1990), Amorphous material in high strain experimental fault gouges, *J. Geophys. Res.*, *95*, 15,589–15,602, doi:10.1029/JB095iB10p15589.